Dual-Function Radar-Communication System Aided by Intelligent Reflecting Surfaces

Yikai Li
School of Computing
Southern Illinois University
Carbondale, IL, USA
yikai.li@siu.edu

Athina Petropulu
Dept. of Electrical and Computer Engineering
Rutgers University
Piscataway, NJ, USA
athinap@rutgers.edu

arXiv:2204.04721v1 [eess.SP] 10 Apr 2022

***Abstract*—We propose a novel design of a dual- function radar-communication (DFRC) system aided by an Intelligent Reflecting Surface (IRS). We consider a scenario with one target and multiple communication receivers, where there is no line-of-sight between the radar and the target. The radar precoding matrix and the IRS weights are optimally designed to maximize the weighted sum of the signal-to-noise ratio (SNR) at the radar receiver and the SNR at the communication receivers subject to power constraints and constant modulus constraints on the IRS weights. The problem is decoupled into two sub-problems, namely, waveform design and IRS weight design, and is solved via alternating optimization. The former subproblem is solved via linear programming, and the latter via manifold optimization with a quartic polynomial objective. The key contribution of this paper lies in solving the IRS weight design sub-problem that is based on the optimization of a quartic objective function in the IRS weights, and is subject to unit modulus-constraint on the IRS weights. Simulation results are provided to show the convergence behavior of the proposed algorithm under different system configurations, and the effectiveness of using IRS to improve radar and communication performance.**

***Index Terms*—DFRC, IRS, joint optimization, manifold optimization**

I. Introduction

Dual-function radar-communication (DFRC) systems offer sensing and communication functionality out of a single platform and using the same waveform. As such, they efficiently use the spectrum and also offer smaller device size and lower hardware cost as compared to systems that perform sensing and communication out of separate platforms [1]. Several works have focused on the design of DFRC systems that are either radar-centric, or communication-centric, and have considered joint designs [2], [3] and [4].

Intelligent reflecting surface (IRS) technology has been gaining a lot of ground for the design of next generation communication systems [5]. Low-cost IRS platforms can be deployed in the path of the signal to change the signal's propagation characteristics. By controlling the amplitudes and/or phases of the responses of the individual IRS elements, the IRS can implement fine-grained passive beamforming for directional signal nulling or enhancement [6].

While there is significant body of literature on reaping the benefits of IRS for wireless communication systems [5], [6], the use of IRS in radar is only now starting to receive attention [7]–[11]. A smart IRS can enhance the power of the reflected target signal, or the signal-to-noise ratio (SNR) at the receive array, and thus improve the target detection performance [7]–[9]. In [7], the radar transmits/receives through two separate beams, one pointing towards the search direction and the other towards the IRS. The smart IRS can be controlled to focus the impinging wavefront towards the radar during the reception stage, or towards the target during the transmission stage. The IRS can also be placed near the radar to fill the area covered by the radar beam, which essentially plays the role of a feed antenna [7]. A radar with a far-away placed IRS can form a low-cost bistatic radar system, offering additional diversity gain [7]. Using multiple distributed IRS platforms can lead to sharper main lobe and more accurate angle estimation, better angle resolution, and higher detection probability [8], [9]. The IRS can also help mitigate the interference between spectrum sharing systems [10], or used for non-line of sight (N-LOS) radar surveillance [11], [12]. Each IRS element induces a phase shift ϕ on the incident signal, thus the responses of the elements, or IRS weights, have unit magnitude.

Although the effectiveness of IRS on independent radar or communication systems has been studied, research on the effectiveness of IRS in integrated DFRC systems is still in early stages [13], [14]. In [13], the design of an IRS-aided DFRC is based on jointly minimizing the radar beampattern error and the communication multi-user interference by alternatively optimizing the radar precoding matrix and IRS weights. In that case, the objective function is a quadratic polynomial in the IRS weight matrix. In [14], the design is based on radar SNR maximization subject to a communication receiver SNR constraint. The objective function of [14] is quartic in the IRS weight matrix. The IRS design problem is relaxed into a semi-definite programming (SDP) problem by dropping the unit modulus IRS weight constraint, and is then solved using semi-definite relaxation (SDR) techniques. However, a rank-one solution is hard to obtain and the algorithm convergence cannot be guaranteed with the Gaussian randomization approximation method [14].

In this paper we consider an IRS aided DFRC system, for a scenario in which there is one target and multiple communication receivers. There is no line-of-sight between the radar and the target, and target detection is carried out based on signals reflected by the IRS. We propose a novel co-design of

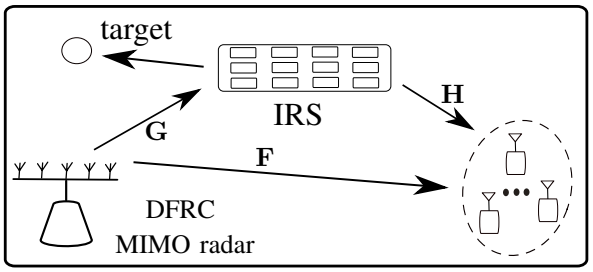


Fig. 1. Intelligent reflecting surface assisted DFRC system.

IRS weights and radar waveform for maximizing the weighted sum of the received SNR at the radar and communication receivers based on constant modulus constraints on the IRS weights. The optimization problem is formulated as alternating optimization of two sub-problems, namely, radar waveform design and IRS weight design. The first problem is solved via linear programming, and the second via manifold optimization with a quartic polynomial objective function with respect to the IRS weights. Derivation of the gradient of the quartic objective function is more challenging than that of a typical quadratic objective function. For this we borrow ideas from the work in [15], which focuses on a different scenario, namely, a disturbance power minimization problem at the output of the matched filter in a single antenna cognitive radar. Our proposed method allows us to deal with both the unit modulus IRS weight constraint and a quartic objective function, and this is something that has not been explored in [13], [14].

The closest work on DFRC to this paper is [14], which also considers improving the SNR for the radar and communication receivers under a radar transmit power budget. However, in [14], the highly non-convex constant-modulus constraint for the IRS weights is relaxed during the optimization process, leading to less accurate solution and slower algorithm convergence. Due to the constant-modulus constraint, the solution is constrained onto a complex circle manifold, and thus solutions obtained in Euclidean space will deviate from that manifold. The work of [14] uses Gaussian randomization, i.e., it relaxes the constraint and then generates randomized solutions and picks the one which maximizes the objective function. However, this approach is not efficient since it requires a large number of realizations to get an accurate enough solution. The work of [13] is also related to our work, except that the design criterion is different, leading to a different optimization problem.

Notation: $\mathbf{M}^H$, $\mathbf{M}^*$, and $\mathbf{M}_{k,l}$ are the conjugate-transpose, conjugate, and the (k,l)-th element of a matrix $\mathbf{M}$, respectively. $\mathbb{E}[X]$ and $\mathbb{V}\mathrm{ar}[X]$ are the mean and variance of a random variable X, respectively. $\mathrm{tr}[\mathbf{M}]$ denotes the trace of a square matrix $\mathbf{M}$. In addition, $\mathbf{0}_{m\times n}$ and $\mathbf{I}_m$ respectively denote an $m \times n$ matrix with all zero elements and an $m\times m$ identity matrix. Moreover, $\otimes$ and $\circ$ are respectively the Kronecker product operator and Hadamard product operator. $\mathbf{v} \sim \mathcal{CN}(\mathbf{0}_{m\times 1}, \sigma^2\mathbf{I}_m)$ represents that $\mathbf{v}$ is an $m\times 1$ circularly symmetric complex Gaussian vector with zero mean and covariance matrix $\sigma^2\mathbf{I}_m$.

II. System model

Let us consider an IRS-aided DFRC system (Fig. 1), consisting of a MIMO radar with an M-antenna uniform linear array (ULA) as transmitter, and an M-antenna ULA receive array, both with antenna spacing d. There are K single-antenna communication receivers and one point target. The DFRC is aided by an IRS platform, modeled as an N-element uniform planar array (UPA), with N_x elements per row and N_y per column. We assume that there exists no line of sight (LOS) between the radar and target. All channels are assumed to be flat fading and perfectly known.

The signal transmitted by the radar can be written as

$$\mathbf{X} = \mathbf{W}\mathbf{s}, \tag{1}$$

where $\mathbf{W} \in \mathbb{C}^{M\times M}$ and $\mathbf{s} \in \mathbb{C}^{M\times 1}$ respectively represent the radar precoding matrix and signal vector intended for the communication users. Radar transmit signal which is reflected by the IRS, then by the target, and the target echo arrives at the radar receiver via the IRS (since there is no direct path between the radar and the target). The received signal equals

$$\begin{aligned}\mathbf{r}_r &= \eta\mathbf{G}^T\mathbf{\Theta}\mathbf{a}_R(\phi_h,\phi_v)\mathbf{a}_R^T(\phi_h,\phi_v)\mathbf{\Theta}\mathbf{G}\mathbf{W}\mathbf{s} + \mathbf{n}_r \\ &= \mathbf{F}_r\mathbf{W}\mathbf{s} + \mathbf{n}_r,\end{aligned} \tag{2}$$

where η is the complex channel coefficient corresponding to the radar-IRS-target-IRS-radar path; $\mathbf{a}_R(\phi_h,\phi_v) = \mathbf{a}_{R_y}(\phi_h,\phi_v)\otimes\mathbf{a}_{R_x}(\phi_h,\phi_v)$ is the steering vector of the IRS where $\mathbf{a}_{R_y}(\phi_h,\phi_v) = [1,\ e^{j2\pi d\cos\phi_h\sin\phi_v/\lambda},\ \cdots,\ e^{j2\pi(N_y-1)d\cos\phi_h\sin\phi_v/\lambda}]^T$ and $\mathbf{a}_{R_x}(\phi_h,\phi_v)$ similarly defined based on N_x; ϕ_h and ϕ_v are respectively the angles of the target relative the IRS in the azimuth and elevation planes; $\mathbf{\Theta} = \mathrm{diag}([e^{j\theta_1},\cdots,e^{j\theta_N}])$ is the phase shift matrix of the IRS, θ_n is the delivered phase shift of the n-th IRS element for $n \in \{1,\cdots,N\}$ and $N = N_xN_y$ is the total number of IRS elements; $\mathbf{G}$ is the channel between the radar and the IRS elements, and $\mathbf{n}_r \sim \mathcal{CN}(\mathbf{0}_{M\times 1}, \sigma_r^2\mathbf{I}_M)$ models the additive white Gaussian noise (AWGN) at the radar receiver where σ_r^2 is the average noise power per radar receiver antenna.

The signal reaches the communication receivers through a direct path also through signal reflected by the IRS. Received signal at the communication receivers can be written as

$$\mathbf{r}_c = (\mathbf{F} + \mathbf{H}\mathbf{\Theta}\mathbf{G})\,\mathbf{W}\mathbf{s} + \mathbf{n}_c = \mathbf{F}_c\mathbf{W}\mathbf{s} + \mathbf{n}_c, \tag{3}$$

where $\mathbf{F}$ is channel between the radar and the communication receivers, and $\mathbf{H}$ channel between the IRS and the communication receivers, and $\mathbf{n}_c \sim \mathcal{CN}(\mathbf{0}_{K\times 1}, \sigma_c^2\mathbf{I}_K)$ models the AWGN at the communication receivers where σ_c^2 is the average noise power per single-antenna communication receiver.

The output SNRs at the radar and communication receivers can be respectively written as

$$\gamma_r = \mathbb{E}\left[\mathrm{tr}\left[\mathbf{r}_r\mathbf{r}_r^H\right]\right]/\sigma_r^2 = \mathrm{tr}\left[\mathbf{F}_r\mathbf{W}\mathbf{W}^H\mathbf{F}_r^H\right]/\sigma_r^2, \tag{4}$$

$$\gamma_c = \mathbb{E}\left[\mathrm{tr}\left[\mathbf{r}_c\mathbf{r}_c^H\right]\right]/\sigma_c^2 = \mathrm{tr}\left[\mathbf{F}_c\mathbf{W}\mathbf{W}^H\mathbf{F}_c^H\right]/\sigma_c^2. \tag{5}$$

III. System Design

We will design the precoder matrix $\mathbf{W}$, and the IRS phase shift matrix $\mathbf{\Theta}$, so that we optimize a weighted combination

of the radar received SNR and that delivered at the communication system, with α being a weight, i.e.,

$$\max_{\mathbf{W},\boldsymbol{\Theta}} \quad (1-\alpha)\gamma_r + \alpha\gamma_c \tag{6a}$$
$$\text{s.t.} \quad |\boldsymbol{\Theta}_{n,n}| = 1, \ \ \forall n \in \{1,\cdots,N\} \tag{6b}$$
$$\text{tr}\big[\mathbf{W}\mathbf{W}^H\big] = P_0 \tag{6c}$$
$$\|\mathbf{W}\mathbf{W}^H - \mathbf{R}_d\| \leq \gamma_{bp} \tag{6d}$$

where (6b) is the unit modulus constraint for the IRS phase shift matrix $\boldsymbol{\Theta}$ and $\boldsymbol{\Theta}_{n,n}$ denotes the n-th diagonal element of the square matrix $\boldsymbol{\Theta}$, (6c) represents the total transmit power constraint at the radar, P_0 is the radar power budget, and (6d) indicates that the beam pattern deviation from a desired one should be within γ_{bp} from a pre-defined threshold. Here, $\mathbf{R}_d$ is the covariance matrix of the desired waveform.

The optimization problem of (6) is highly non-convex. However, it can be efficiently solved via decomposed into two sub-problems, to be solved in an alternating way. Specifically, the first sub-problem can be defined as maximizing the objective function by solving for the precoder matrix $\mathbf{W}$, taking the IRS phase shift matrix $\boldsymbol{\Theta}$ as constant. The second problem can be defined as solving for $\boldsymbol{\Theta}$ by taking $\mathbf{W}$ as constant. These two sub-problems are being solved alternatingly until the objective function converges.

Sub-problem 1. The first sub-problem optimizes the objective function with respect to $\mathbf{W}$ for fixed $\boldsymbol{\Theta}$. The objective function can be written as $f(\mathbf{W}) = (1-\alpha)\text{tr}\big[\mathbf{W}\mathbf{W}^H\mathbf{F}_r^H\mathbf{F}_r\big]/\sigma_r^2 + \alpha\text{tr}\big[\mathbf{W}\mathbf{W}^H\mathbf{F}_c^H\mathbf{F}_c\big]/\sigma_c^2 = \text{tr}\big[\mathbf{W}\mathbf{W}^H\mathbf{C}\big]$, where $\mathbf{C} = (1-\alpha)\mathbf{F}_r^H\mathbf{F}_r/\sigma_r^2 + \alpha\mathbf{F}_c^H\mathbf{F}_c/\sigma_c^2$. Thereby, the sub-problem 1 can be written as

$$\max_{\mathbf{W}} \quad \text{tr}\Big[\mathbf{W}\mathbf{W}^H\mathbf{C}\Big] \tag{7a}$$
$$\text{s.t.} \quad \text{tr}\Big[\mathbf{W}\mathbf{W}^H\Big] = P_0 \tag{7b}$$
$$\|\mathbf{W}\mathbf{W}^H - \mathbf{R}_d\| \leq \gamma_{bp} \tag{7c}$$

This is a linear programming problem with variable $\mathbf{W}\mathbf{W}^H$. Then, the precoder matrix $\mathbf{W}$ can be computed as the square root matrix of $\mathbf{W}\mathbf{W}^H$.

Sub-problem 2. In the second sub-problem, we use the value of $\mathbf{W}$ obtained in sub-problem 1, and optimize with respect to $\boldsymbol{\Theta}$. The objective function $f = \text{tr}\big[\mathbf{W}\mathbf{W}^H\mathbf{C}\big]$ can be re-written as a function of $\boldsymbol{\Theta}$ by expressing $\mathbf{C}$ in terms of $\mathbf{F}_r = \eta\mathbf{G}^T\boldsymbol{\Theta}\mathbf{a}_R(\phi_h,\phi_v)\mathbf{a}_R^T(\phi_h,\phi_v)\boldsymbol{\Theta}\mathbf{G}$ and $\mathbf{F}_c = \mathbf{F} + \mathbf{H}\boldsymbol{\Theta}\mathbf{G}$, i.e.,

$$f(\boldsymbol{\Theta}) = t_4 + t_2 + t_1 + t_0, \tag{8}$$

where t_4, t_2, t_1 and t_0 are respectively the quartic, quadratic, linear and constant terms with regard to $\boldsymbol{\Theta}$, defined as

$$t_4 = (1-\alpha)\eta^2\text{tr}\Big[\mathbf{G}^T\boldsymbol{\Theta}\mathbf{R}\boldsymbol{\Theta}\mathbf{G}\mathbf{W}\mathbf{W}^H\mathbf{G}^H\boldsymbol{\Theta}^H\mathbf{R}^H\boldsymbol{\Theta}^H\mathbf{G}^*\Big]/\sigma_r^2, \tag{9a}$$
$$t_2 = \alpha\text{tr}\Big[\mathbf{W}\mathbf{W}^H\mathbf{G}^H\boldsymbol{\Theta}^H\mathbf{H}^H\mathbf{H}\boldsymbol{\Theta}\mathbf{G}\Big]/\sigma_c^2, \tag{9b}$$
$$t_1 = \alpha\Big(\text{tr}\Big[\mathbf{W}\mathbf{W}^H\mathbf{G}^H\boldsymbol{\Theta}^H\mathbf{H}^H\mathbf{F}\Big] + \text{tr}\Big[\mathbf{W}\mathbf{W}^H\mathbf{F}^H\mathbf{H}\boldsymbol{\Theta}\mathbf{G}\Big]\Big)/\sigma_c^2, \tag{9c}$$
$$t_0 = \alpha\text{tr}\Big[\mathbf{W}\mathbf{W}^H\mathbf{F}^H\mathbf{F}\Big]/\sigma_c^2, \tag{9d}$$

where $\mathbf{R} = \mathbf{a}_R(\phi_h,\phi_v)\mathbf{a}_R^T(\phi_h,\phi_v)$.

The term t_0 is not a function of $\boldsymbol{\Theta}$, thus can be safely discarded. Thereby, sub-problem 2 can be re-formulated as

$$\max_{\boldsymbol{\Theta}} \quad t_4 + t_2 + t_1 \tag{10a}$$
$$\text{s.t.} \quad |\boldsymbol{\Theta}_{n,n}| = 1, \ \ \forall n \in \{1,\cdots,N\} \tag{10b}$$

To make the objective function more mathematical tractable, the quartic term t_4 can be re-written in vector form as

$$t_4 = (1-\alpha)(\eta^2/\sigma_r^2)\sum_{i=1}^{M}\sum_{j=1}^{M} h_{ij}(\boldsymbol{\theta})h_{ij}^*(\boldsymbol{\theta}), \tag{11}$$

where $h_{ij}(\boldsymbol{\theta}) = \boldsymbol{\theta}^T[\mathbf{R}\circ(\mathbf{G}\mathbf{w}_j\mathbf{g}_i^T)^T]\boldsymbol{\theta}$, $\boldsymbol{\theta} = \boldsymbol{\Theta}\mathbf{1}_{N\times 1}$, $\mathbf{w}_j$ is the j-th column of $\mathbf{W}$, and $\mathbf{g}_i$ is the i-th column of $\mathbf{G}$. Meanwhile the quadratic term t_2 can be re-arranged as

$$t_2 = \boldsymbol{\theta}^H\mathbf{D}_1\boldsymbol{\theta}, \tag{12}$$

where $\mathbf{D}_1 = (\alpha/\sigma_c^2)(\mathbf{H}^H\mathbf{H})\circ(\mathbf{G}\mathbf{W}\mathbf{W}^H\mathbf{G}^H)^T$.

Similarly, t_1 can be re-written as

$$t_1 = \boldsymbol{\theta}^H\mathbf{v}^* + \boldsymbol{\theta}^T\mathbf{v}, \tag{13}$$

where $\mathbf{v} = \Big[(\mathbf{D}_2)_{1,1},\cdots,(\mathbf{D}_2)_{N,N}\Big]^T$, and $\mathbf{D}_2 = (\alpha/\sigma_c^2)\mathbf{G}\mathbf{W}\mathbf{W}^H\mathbf{F}^H\mathbf{H}$. Thus, the sub-problem 2 can be concisely re-written as

$$\max_{\boldsymbol{\theta}} \quad f_1(\boldsymbol{\theta}) = t_4(\boldsymbol{\theta}) + t_2(\boldsymbol{\theta}) + t_1(\boldsymbol{\theta}) \tag{14a}$$
$$\text{s.t.} \quad |\boldsymbol{\theta}_{n,1}| = 1, \ \ \forall n \in \{1,\cdots,N\} \tag{14b}$$

where $\boldsymbol{\theta}_{n,1}$ is the n-th element of the column vector $\boldsymbol{\theta}$. The constraint in (14b) defines a complex circle manifold. So, the second sub-problem has been re-formulated as an optimization problem with a quartic polynomial objective function constrained by an oblique manifold, which can be efficiently solved by a standard oblique manifold optimization method as follows.

Let us define the oblique manifold based on the unit modulus constraint of (14b)

$$\mathcal{O} = \{\boldsymbol{\theta} \in \mathbb{C}^N | [\boldsymbol{\theta}\boldsymbol{\theta}^H]_{n,n} = 1, \forall n = 1,\cdots,N\}. \tag{15}$$

The tangent space of $\mathcal{O}$ at a certain point $\boldsymbol{\theta}_j \in \mathbb{C}^N$ can be written in a set form as

$$T_{\boldsymbol{\theta}_j}\mathcal{O} = \{\mathbf{x} \in \mathbb{C}^N | \text{Re}\{\mathbf{x}\circ\boldsymbol{\theta}_j^*\} = \mathbf{0}_{N\times 1}\}. \tag{16}$$

The Euclidean gradient of the re-arranged objective function $f_1(\boldsymbol{\theta})$ in (14a) can be derived as

$$\nabla f_1(\boldsymbol{\theta}) = (1-\alpha)\eta^2/\sigma_r^2\sum_{i=1}^{M}\sum_{j=1}^{M}[(\mathbf{Z}_{ij} + \mathbf{Z}_{ij}^T)\boldsymbol{\theta}\boldsymbol{\theta}^H\mathbf{Z}_{ij}^*\boldsymbol{\theta}^*$$
$$+(\mathbf{Z}_{ij}^* + \mathbf{Z}_{ij}^H)\boldsymbol{\theta}^*\boldsymbol{\theta}^T\mathbf{Z}_{ij}\boldsymbol{\theta}] + 2\mathbf{D}_1\boldsymbol{\theta} + 2\mathbf{v}, \tag{17}$$

where $\mathbf{Z}_{ij} = \mathbf{R}\circ(\mathbf{G}\mathbf{w}_j\mathbf{g}_i^T)^T$. Readers can refer to [15] for the derivation of gradient of $t_4(\boldsymbol{\theta})$. As we all know, the Euclidean gradient is the direction in which the objective function increases fastest. However, with the complex circle manifold constraint, we are not able to directly use the Euclidean gradient as the search direction, which should be in the tangent space of the manifold $\mathcal{O}$ at a certain point $\boldsymbol{\theta}_j$, i.e. $T_{\boldsymbol{\theta}_j}\mathcal{O}$. Thus we calculate the projection of the Euclidean gradient onto $T_{\boldsymbol{\theta}_j}\mathcal{O}$ instead as search direction as follows [16]

$$\text{grad}_{\boldsymbol{\theta}_j} f_1 = \nabla f_1(\boldsymbol{\theta}_j) - \text{Re}\{\nabla f_1(\boldsymbol{\theta}_j)\circ\boldsymbol{\theta}_j^*\}\circ\boldsymbol{\theta}_j. \tag{18}$$

This is also known as the Riemannian gradient, which is a tangent vector of $\mathcal{O}$ at $\boldsymbol{\theta}_j$, the direction in which the objective function increases fastest.

We denote the variable to be optimized $\boldsymbol{\theta}$ in the j-th iteration as $\boldsymbol{\theta}_j$. To find the value of $\boldsymbol{\theta}$ in the $(j+1)$-th iteration which

is $\boldsymbol{\theta}_{j+1}$, we first let $\boldsymbol{\theta}_{j+1} = \boldsymbol{\theta}_j + \delta_j \text{grad}_{\boldsymbol{\theta}_j} f_1$ where δ_j is the step size and $\text{grad}_{\boldsymbol{\theta}_j} f_1$ is the search direction. In this case, $\boldsymbol{\theta}_{j+1}$ will be no longer on the complex circle manifold $\mathcal{O}$, so a retraction operation is needed which normalizes $\boldsymbol{\theta}_{j+1}$ element-wisely to retract $\boldsymbol{\theta}_{j+1}$ back onto $\mathcal{O}$, i.e.

$$\boldsymbol{\theta}_{j+1} = (\boldsymbol{\theta}_j + \delta_j \text{grad}_{\boldsymbol{\theta}_j} f_1) \circ \frac{1}{|\boldsymbol{\theta}_j + \delta_j \text{grad}_{\boldsymbol{\theta}_j} f_1|}. \quad (19)$$

For the sake of exposition, the overall algorithm for solving the alternating optimization of radar precoder matrix $\mathbf{W}$ and IRS phase shift matrix $\boldsymbol{\Theta}$ is given in Algorithm 1. In addition, ε in Algorithm 1 is an error tolerance indicator. Algorithm 1 is essentially the same with the methodology of [13] which is manifold optimization based alternating optimization. However, our objective here is SNR maximization, which is a quartic function in $\boldsymbol{\Theta}$, while the objective of [13] is beampattern deviation and multi-user interference minimization which is a quadratic function in $\boldsymbol{\Theta}$.

Algorithm 1: Complex circle manifold constrained iterative weighted received SNR maximization

Result: Return $\mathbf{W}$ and $\boldsymbol{\Theta}$.
Initialization: $\boldsymbol{\Theta} = \boldsymbol{\Theta}_0$, $\boldsymbol{\theta}_0 = \boldsymbol{\Theta}_0 \mathbf{1}_{N\times 1}$, $j = 0$;
while $\left(j < j_{\max} \;\&\&\; \left|\left[f_1^{(j)} - f_1^{(j-1)}\right]/f_1^{(j-1)}\right| > \varepsilon\right)$ **do**
  Solve the problem of (7) for $\mathbf{W}$.
  Calculate Euclidean gradient $\nabla f_1(\boldsymbol{\theta}_j)$ based on (17);
  Compute Riemannian gradient $\text{grad}_{\boldsymbol{\theta}_j} f_1$ as (18);
  Update $\boldsymbol{\theta}_j$ to $\boldsymbol{\theta}_{j+1}$ as (19);
  $j = j + 1$;
  $\boldsymbol{\Theta} = \text{diag}(\boldsymbol{\theta}_{j+1})$;
end

IV. NUMERICAL RESULTS

We present numerical results to demonstrate the convergence of the proposed method, and quantify the advantages of the IRS-aided DFRC system. The channels $\mathbf{F}$ and $\mathbf{H}$ are simulated as flat Rayleigh fading and $\mathbf{G}$ is Rician.

Fig. 2 shows the convergence rate of the proposed weighted sum received SNR maximization algorithm for different values of the weighting parameter (α). Solid lines indicate the mean of SNR gain over 20 iterations, and the shaded area around the mean are bounded by the mean plus or minus standard deviation, indicating variance between different runs. It can be observed from Fig. 2 that a smaller α leads to faster convergence. It should be noted that the radar SNR is a quartic function of the IRS phase shift matrix ($\boldsymbol{\Theta}$), while that for communication users is quadratic into $\boldsymbol{\Theta}$. Therefore the radar SNR is more sensitive to the change of $\boldsymbol{\Theta}$, and the radar SNR increases faster with regard to iteration number. Smaller α assigns larger weight for radar SNR, and the weighted SNR increases faster in this scenario.

In Fig. 3, the relationship between the weighted received SNR and transmit SNR is displayed. The weighted received SNR can be boosted by increasing the number of radar antennas (M), the number of IRS elements (N), or the transmit SNR/power budget P_0. Therefore, the usefulness of IRS deployment for the DFRC system is quantified.

TABLE I
SIMULATION PARAMETERS

Parameter	Value
Iterative algorithm error tolerance ε (dB)	-30
Maximum number of iterations $j_{\max}$	500
Iterative algorithm step size δ_j	10^{-1}
Number of communication receivers	5
Rician factor of $\mathbf{G}$ channel K_G (dB)	0
Radar receive array adjacent antenna distance	0.5λ
Radar transmit array adjacent antenna distance	0.5λ
Radar beampattern deviation threshold γ_{bp} (dB)	10
Average noise power per radar receiver antenna σ_r^2 (dB)	0
Average noise power per communication receiver antenna σ_c^2 (dB)	0

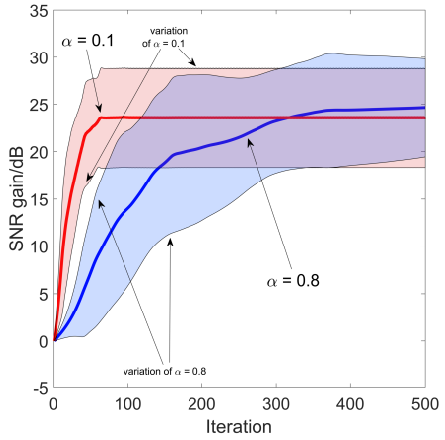


Fig. 2. Rate of convergence of the proposed alternating algorithm. System parameters: $P_0 = 30$ dBm, $M = 8$, $N = 64$.

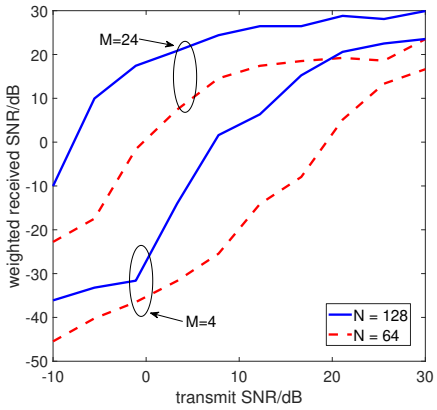


Fig. 3. Weighted received SNR versus transmit SNR at the radar. System parameters: $\alpha = 0.5$.

V. CONCLUSIONS

We have proposed a novel IRS-aided DFRC system design and a manifold optimization based alternating optimization algorithm to maximize the weighted sum received SNR while considering the constant modulus constraint for IRS weights. The simulations have validated the convergence of the proposed optimization algorithm and demonstrated the advantage of exploiting IRS in the DFRC system to improve the radar and communication performances.

REFERENCES

[1] F. Liu, C. Masouros, A. P. Petropulu, H. Griffiths, and L. Hanzo, "Joint radar and communication design: Applications, state-of-the-art, and the road ahead," *IEEE Trans. Commun.*, vol. 68, no. 6, pp. 3834–3862, 2020.

[2] J. A. Zhang, F. Liu, C. Masouros, R. W. Heath Jr, Z. Feng, L. Zheng, and A. Petropulu, "An overview of signal processing techniques for joint communication and radar sensing," *arXiv preprint arXiv:2102.12780*, 2021.

[3] Z. Xu and A. Petropulu, "A wideband dual function radar communication system with sparse array and OFDM waveforms," *arXiv preprint arXiv:2106.05878*, 2021.

[4] F. Liu, L. Zhou, C. Masouros, A. Li, W. Luo, and A. Petropulu, "Toward dual-functional radar-communication systems: Optimal waveform design," *IEEE Trans. Signal Process.*, vol. 66, no. 16, pp. 4264–4279, 2018.

[5] Q. Wu and R. Zhang, "Towards smart and reconfigurable environment: Intelligent reflecting surface aided wireless network," *IEEE Commun. Mag.*, vol. 58, no. 1, pp. 106–112, 2020.

[6] ——, "Intelligent reflecting surface enhanced wireless network via joint active and passive beamforming," *IEEE Trans. Wireless Commun.*, vol. 18, no. 11, pp. 5394–5409, 2019.

[7] S. Buzzi, E. Grossi, M. Lops, and L. Venturino, "Radar target detection aided by reconfigurable intelligent surfaces," *IEEE Signal Process. Lett.*, vol. 28, pp. 1315–1319, 2021.

[8] W. Lu, B. Deng, Q. Fang, X. Wen, and S. Peng, "Intelligent reflecting surface-enhanced target detection in MIMO radar," *IEEE Sensors Letters*, vol. 5, no. 2, pp. 1–4, 2021.

[9] W. Lu, Q. Lin, N. Song, Q. Fang, X. Hua, and B. Deng, "Target detection in intelligent reflecting surface aided distributed MIMO radar systems," *IEEE Sensors Letters*, vol. 5, no. 3, pp. 1–4, 2021.

[10] X. Wang, Z. Fei, J. Guo, Z. Zheng, and B. Li, "RIS-assisted spectrum sharing between MIMO radar and MU-MISO communication systems," *IEEE Wireless Commun. Lett.*, vol. 10, no. 3, pp. 594–598, 2021.

[11] A. Aubry, A. De Maio, and M. Rosamilia, "Reconfigurable intelligent surfaces for N-LOS radar surveillance," *IEEE Trans. Veh. Technol.*, pp. 1–1, 2021.

[12] F. Wang, H. Li, and J. Fang, "Joint active and passive beamforming for IRS-assisted radar," *IEEE Signal Process. Lett.*, pp. 1–1, 2021.

[13] X. Wang, Z. Fei, Z. Zheng, and J. Guo, "Joint waveform design and passive beamforming for RIS-assisted dual-functional radar-communication system," *IEEE Trans. Veh. Technol.*, vol. 70, no. 5, pp. 5131–5136, 2021.

[14] Z.-M. Jiang, M. Rihan, P. Zhang, L. Huang, Q. Deng, J. Zhang, and E. M. Mohamed, "Intelligent reflecting surface aided dual-function radar and communication system," *IEEE Syst. J.*, pp. 1–12, 2021.

[15] K. Alhujaili, V. Monga, and M. Rangaswamy, "Quartic gradient descent for tractable radar slow-time ambiguity function shaping," *IEEE Transactions on Aerospace and Electronic Systems*, vol. 56, no. 2, pp. 1474–1489, 2020.

[16] ——, "Transmit MIMO radar beampattern design via optimization on the complex circle manifold," *IEEE Trans. Signal Process.*, vol. 67, no. 13, pp. 3561–3575, 2019.